

Hadron-string cascade versus hydrodynamics in Cu + Cu collisions at $\sqrt{s_{NN}} = 200$ GeV

T. Hirano,¹ M. Isse,² Y. Nara,³ A. Ohnishi,² and K. Yoshino²

¹ *Department of Physics, Columbia University, New York, NY 10027*

² *Division of Physics, Graduate School of Science,*

Hokkaido University, Sapporo, Hokkaido 060-0810, Japan

³ *Institut für Theoretische Physik, Johann Wolfgang Goethe-Universität,
Max-von-Laue-Str. 1, 60438 Frankfurt am Main, Germany*

Single particle spectra as well as elliptic flow in Cu+Cu collisions at $\sqrt{s_{NN}} = 200$ GeV are investigated within a hadronic cascade model and an ideal hydrodynamic model. Pseudorapidity distribution and transverse momentum spectra for charged hadrons are surprisingly comparable between these two models. However, a large deviation is predicted for the elliptic flow. The forthcoming experimental data will clarify the transport and thermalization aspects of matter produced in Cu+Cu collisions.

PACS numbers: 24.10.Lx, 24.10.Nz, 25.75.Ld, 25.75.-q

One of the primary current interests in the Relativistic Heavy Ion Collider (RHIC) experiments is to explore the properties of QCD matter far from stable nuclei, especially the confirmation of the deconfined and thermalized matter, *i.e.* the quark gluon plasma (QGP), which has been predicted from the lattice QCD calculations [1]. While high and medium p_T observables such as the parton energy loss [2] and coalescence behavior of hadron elliptic flows [3] are generally believed to give strong evidences of high dense matter formation, hadrons at these momenta are not necessarily formed from thermalized matter. Therefore, low p_T observables are also important to confirm whether *equilibrium* is achieved or not.

Elliptic flow is one of the promising observables to study the QCD matter produced in heavy ion collisions since it is believed to be sensitive to the properties of the matter at initial stages and the collision geometry. Indeed, incident energy as well as impact parameter dependences of elliptic flow have been investigated extensively. Elliptic flow, *i.e.* the momentum anisotropy with respect to the reaction plane $v_2 = \langle \cos(2\phi) \rangle$, has been measured in a wide energy range from GSI-SIS ($E_{\text{inc}} \lesssim 1A$ GeV) [4], BNL-AGS ($E_{\text{inc}} = 2 - 11A$ GeV) [5], to CERN-SPS ($E_{\text{inc}} = 40 - 158A$ GeV) [6], in addition to BNL-RHIC [7]. Measured collective flows are well reproduced by nuclear transport models assuming the momentum dependent nuclear mean-field at SIS to AGS ($E_{\text{inc}} \simeq 0.2 - 11A$ GeV) [8, 9] and SPS ($E_{\text{inc}} = 40, 158A$ GeV) [10] energies, whereas elliptic flow at RHIC at mid-rapidity is underestimated in nonequilibrium transport models which do not include explicit partonic interactions [11–13]. It is also reported that hadronic models explain elliptic flow only at low transverse momentum $p_T \lesssim 1$ GeV/c at RHIC [14, 15]. Partonic interactions followed by quark coalescence hadronization mechanism are proposed in Ref. [16] to account for the experimental data on elliptic flow. Note, however, that hadronic cascade models reproduce elliptic flow in forward/backward rapidity regions at RHIC.

On the other hand, in Au+Au collisions at RHIC energies the magnitude of v_2 and its transverse momentum p_T

and mass m dependences are close to predictions based on ideal and non-dissipative hydrodynamics simulations around midrapidity ($|\eta| \lesssim 1$), in the low transverse momentum region ($p_T \lesssim 1$ GeV/c), and up to semicentral collisions ($b \lesssim 5$ fm) [17, 18]. This is one of the main results which leads to a recent announcement of the discovery of perfect fluidity at RHIC [19]. (See Ref. [20] for recent reinterpretation of the RHIC data based on current hydrodynamic results.) Despite the apparent success near midrapidity at RHIC, ideal hydrodynamics overestimates the data at lower incident energies (SIS, AGS and SPS) as well as in forward/backward rapidity regions at RHIC probably due to the lack of dissipative effects.

We study Cu+Cu collisions at RHIC in the present work, which is a complementary study of elliptic flow in Au+Au collisions. The particle density and the size of the system are smaller in Cu+Cu collisions than in Au+Au collisions. So the reasonable agreement of hydrodynamic results with Au+Au data may be spoiled in Cu+Cu collisions and a non-equilibrium hadronic description can be relatively important even at RHIC energies. Therefore we employ both a hadronic transport model JAM and a hydrodynamic model to make predictions for elliptic flow in Cu+Cu collisions. Below we briefly summarize hadron-string cascade JAM [21] and a hydrodynamic model [22] adopted in this paper.

A hadronic transport model JAM simulates nuclear collisions by the individual hadron-hadron collisions. Soft hadron productions in hadron-hadron scattering are modeled by the resonance and color string excitations. Hard partonic scattering is also included in line with HIJING [23]. Color strings decay into hadrons after their formation time ($\tau \sim 1$ fm/c) according to the Lund string model PYTHIA [24]. Hadrons within their formation time can scatter with other hadrons assuming the additive quark cross section. This simulates constituent quark collisions effectively which is known to be important at SPS energies [25]. Therefore, matter initially created in collisions is represented by the many strings at RHIC, which means that there is no QGP in the model.

Default parameters in JAM are adopted in this work

except for a little wider p_T width in the string decay and a larger partonic minimum p_T ($p_0 = 2.7 \text{ GeV}/c$) to fit charged hadron p_T spectrum in pp collisions at $\sqrt{s_{NN}} = 200 \text{ GeV}$. In addition to hadron-hadron collisions, nuclear mean field is incorporated in JAM and its effects are known to be important at AGS and SPS energies [10], but mean field is not expected to play major roles at RHIC. We have thus neglected nuclear mean field in this work. The detailed description of JAM can be found in Ref. [21].

Two of the authors (T.H. and Y.N.) have already developed another dynamical framework to describe three important aspects of relativistic heavy ion collisions [22], namely color glass condensate (CGC) for collisions of two nuclei [26–28], hydrodynamics for space-time evolution of thermalized matter [29], and jet quenching for high p_T non-thermalized partons [30]. Along the line of these works, we use the same model in this study. However, our aim is to study the bulk properties of matter produced in Cu+Cu collisions. In this paper, we neither include jet components in this model nor discuss jet quenching, unlike a series of the previous work [31]. So hydrodynamic results to be presented below include purely boosted thermal components without any semi-hard components.

In Ref. [22], a systematic hydrodynamic analysis in Au+Au collisions at $\sqrt{s_{NN}} = 200 \text{ GeV}$ was performed by using initial conditions taken from the CGC picture for the colliding nuclei. In the conventional hydrodynamic calculations, one chooses initial condition for hydrodynamic equations and thermal freezeout temperature T^{th} so as to reproduce the *observed* particle spectra, such as (pseudo)rapidity distribution and transverse momentum distribution. So it is believed that hydrodynamics has a less predictive power compared with cascade models. However, if the initial particle production at high collisional energies is supposed to be universal as described by the CGC, hydrodynamics with CGC initial conditions can *predict* particle spectra. Here, we employ the IC- n , *i.e.* a prescription that the number density produced in a CGC collision is matched to the hydrodynamic initial condition [22], to obtain the initial distribution of thermodynamic variables at the initial time τ_0 . Once the initial condition is obtained, one solves hydrodynamic equation $\partial_\mu T^{\mu\nu} = 0$ in the three-dimensional Bjorken coordinate (τ, η_s, x, y) [18]. Here we neglect a dissipative effect and a finite (but probably tiny) baryon density. Assuming $N_c = N_f = 3$ massless partonic gas, an ideal gas EOS with a bag constant $B^{1/4} = 247 \text{ MeV}$ is employed in the QGP phase ($T > T_c = 170 \text{ MeV}$). We use a hadronic resonance gas model with all hadrons up to $\Delta(1232)$ mass for later stages ($T < T_c$) of collisions. We take into account chemical freezeout separated from thermal freezeout [32] as required to obtain sufficient yields for heavier particles. Specifically, we assume that chemical freezeout temperature $T^{\text{ch}} = 170 \text{ MeV}$ and kinetic freezeout temperature $T^{\text{th}} = 100 \text{ MeV}$. Note that the slope of p_T spectra becomes insensitive to T^{th} (while v_2 becomes sensitive) when chemical freezeout is taken into

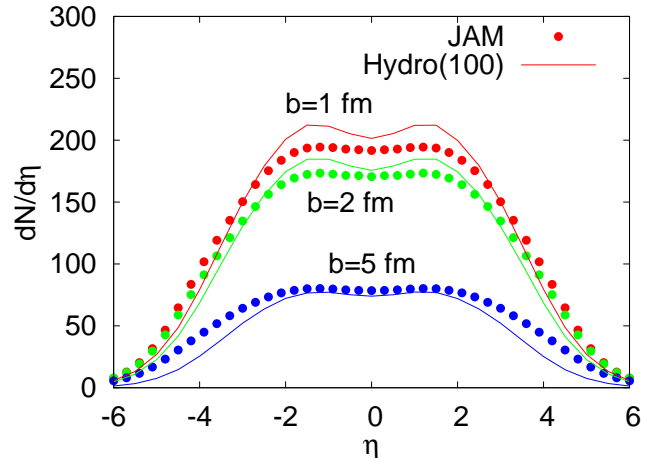


FIG. 1: Pseudorapidity distributions for charged hadrons in Cu+Cu collisions at $\sqrt{s_{NN}} = 200 \text{ GeV}$ for impact parameters $b = 1, 2$, and 5 fm . Circles correspond to the result of JAM. Lines denote the results of hydrodynamics for $T^{\text{th}} = 100 \text{ MeV}$.

account [32]. In the calculation of $v_2(\eta)$, we also use $T^{\text{th}} = 160 \text{ MeV}$ for comparison. If the sQGP core expands as a perfect fluid and the hadronic corona does as a highly dissipative gas as suggested in Ref. [20], the resultant $v_2(\eta)$ and $v_2(p_T)$ are expected to be frozen after hadronization [33, 34] due to the viscous effect. Moreover, T^{th} should be higher for a smaller size of the system [35] as observed in the centrality dependence of the p_T spectra [36]. So the freezeout picture in Cu+Cu collisions can be different from that in Au+Au collisions. In the following predictions for hydrodynamic elliptic flow, we show the results for $T^{\text{th}} = 100$ and 160 MeV . For further details of the hydrodynamic model used in this work, see Refs. [22, 31, 32].

We first compare the bulk single particle spectra between JAM and hydrodynamics. We emphasize again that our hydrodynamic results are insensitive to a choice of T^{th} for transverse and rapidity distributions of charged hadrons. We show results of the pseudorapidity distribution $dN/d\eta$ for charged hadrons in Fig. 1 at impact parameters $b = 1, 2$ and 5 fm . It is seen from this figure that the shape and the magnitude of the distributions from JAM are almost similar to those from hydrodynamics.

In Fig. 2, we compare JAM and hydrodynamic results of the p_T spectra for charged hadrons at impact parameters of $b = 1, 2$ and 5 fm for $|\eta| < 0.33$. Accidentally, these results agree well with each other in transverse momentum range of $p_T < 2 \text{ GeV}/c$. Deviation at higher transverse momentum is due to the lack of jet components in the hydrodynamic simulations.

At least within our models, two distinct pictures, *i.e.* pictures of coherent particle production via CGC combined with sequential sQGP expansion and of transports of secondary hadrons after hadron-hadron collisions summed up by an overlap region of colliding nuclei,

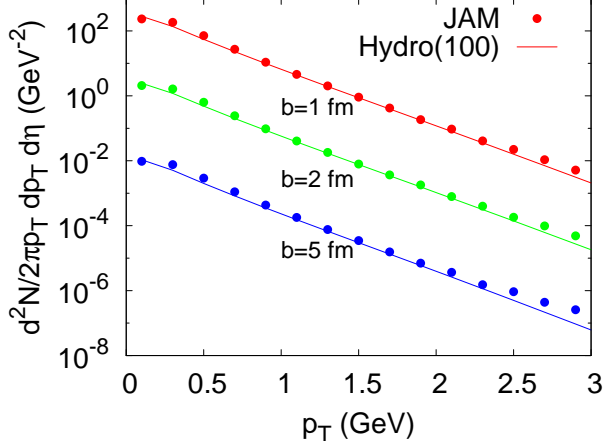


FIG. 2: Comparison of the transverse momentum distributions for charged hadrons between JAM (circles) and hydrodynamics for $T^{\text{th}} = 100$ MeV (lines) at $|\eta| < 0.33$ in Cu+Cu collisions at $\sqrt{s_{NN}} = 200$ GeV. The results for $b=2$ fm (5 fm) are scaled by 10^{-2} (10^{-4}).

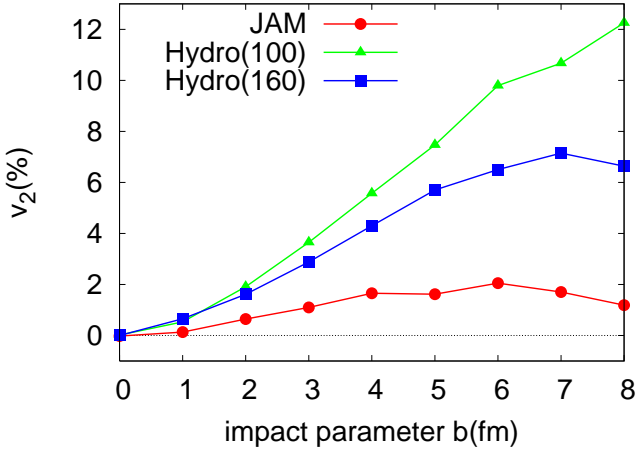


FIG. 3: Elliptic flow v_2 for charged hadrons at mid-rapidity as a function of impact parameter in Cu+Cu collisions at $\sqrt{s_{NN}} = 200$ GeV. Circles connected by lines show the results of JAM. Lines with triangle and square show the results of hydrodynamics with $T^{\text{th}} = 100$ MeV and 160 MeV, respectively.

are indistinguishable in the bulk single hadron distributions in Cu+Cu collisions. Note that free parameters in the “CGC+hydro” model has been fixed by fitting the charged multiplicity in Au+Au collisions at midrapidity. We also note that parameters in JAM are already fixed to fit the data in pp collisions at $\sqrt{s_{NN}} = 200$ GeV.

In Fig. 3, we show the impact parameter b dependence of the elliptic flow v_2 at mid-rapidity for charged hadrons. In the hydrodynamic calculations, kinetic freezeout temperatures $T^{\text{th}} = 100$ MeV and 160 MeV are chosen.

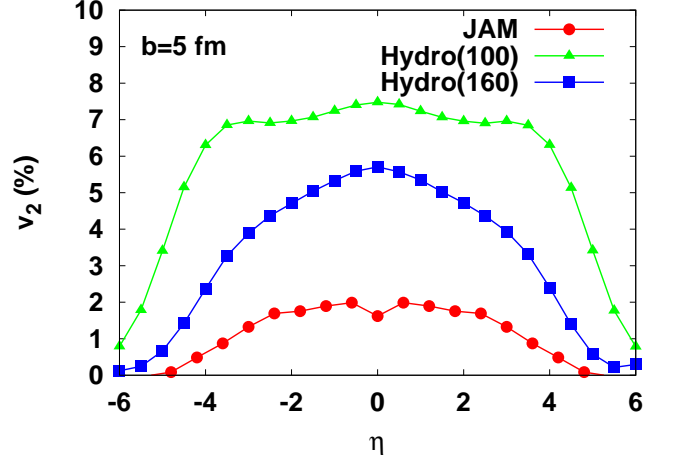


FIG. 4: Elliptic flow v_2 for charged hadrons as a function of pseudorapidity η in Cu+Cu collisions at $\sqrt{s_{NN}} = 200$ GeV at impact parameter $b = 5$ fm. Circles connected by lines show the results of JAM. Lines with triangle and square show the results of hydrodynamics with $T^{\text{th}} = 100$ MeV and 160 MeV, respectively.

While single particle spectra from JAM and hydrodynamics look very similar, a clear difference of $v_2(b)$ is seen: v_2 grows almost linearly with b in hydrodynamics, which is the same as the case in Au+Au collisions, while we find a peak at around $b = 6$ fm in JAM and that the magnitude is only around 20% of the hydrodynamic prediction with $T^{\text{th}} = 100$ MeV. The two distinct pictures within our approach appear differently in the centrality dependence of elliptic flow. Due to the smaller initial energy density in Cu+Cu collisions compared to Au+Au collisions, the spatial anisotropy is still out-of-plane just after the hadronization and v_2 continues to be generated even in the late non-viscous hadronic stage in the ideal hydrodynamic simulation. The data is expected to be comparable with the result for $T^{\text{th}} = 160$ MeV if the initial energy density is large ($e_0 \gg 1$ GeV/fm³) and the equilibration time is small ($\tau_0 \sim 1$ fm/c) enough to create the sQGP phase in Cu+Cu collisions. On the contrary, one expects that it takes more time to reach equilibrium ($\tau_0 > 1$ fm/c) and that the system may not reach the equilibrated sQGP state since the system size and the produced particle number are small compared with those in Au+Au collisions. In that case, the data will be comparable with the result from JAM.

Pseudorapidity dependences of the elliptic flow from JAM and hydrodynamics are compared with each other to understand the longitudinal dynamics in Cu+Cu collisions in Fig. 4. In JAM, we find almost flat behavior of $v_2(\eta)$ around midrapidity ($|\eta| < 2$), where the charged hadron η distribution also shows flat behavior. In JAM, elliptic flow is slowly generated ($t \lesssim 10$ fm) as the hadrons are formed from strings after some formation times [14]. In the hydrodynamic calculations, we show the results

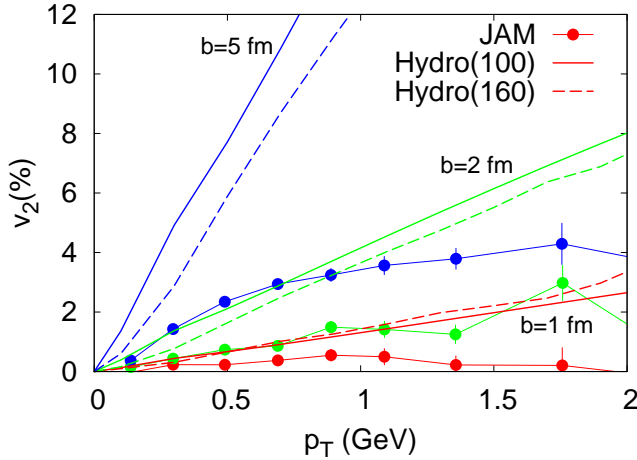


FIG. 5: The calculated elliptic flow v_2 of charged hadrons as a function of transverse momentum p_T for Cu+Cu at $\sqrt{s_{NN}} = 200$ GeV for different impact parameters, $b = 1, 2$, and 5 fm. Circles connected by lines show the results of JAM. Solid and dashed lines show the results of hydrodynamics with $T^{\text{th}} = 100$ MeV and 160 MeV, respectively.

for $T^{\text{th}} = 100$ and 160 MeV, which could be an upper and a lower limit of the *ideal* hydrodynamic prediction respectively. $v_2(\eta)$ for $T^{\text{th}} = 100$ MeV becomes a trapezoidal shape, which looks similar to the result in the previous hydrodynamic study in Au+Au collisions [18, 32]. $v_2(\eta)$ from ideal hydrodynamics for $T^{\text{th}} = 160$ MeV is also shown as a possible result for the situation [20] in which v_2 is generated by the perfect fluid of the sQGP core and is not generated significantly in the dissipative hadronic corona like the result from JAM. Indeed, $v_2(\eta)$ for $T^{\text{th}} = 160$ MeV appears to be a triangle shape which looks similar to the shape in Au+Au data observed by

PHOBOS [37].

In Fig. 5, we compare transverse momentum p_T dependence of elliptic flow for charged hadrons. Hydrodynamic predictions are of course larger than the ones of JAM. In JAM, v_2 starts to be saturated at around 0.8 GeV, and the behavior is qualitatively similar to that in Au+Au collisions and another theoretical prediction in Cu+Cu collisions [38]. It should be noted that we will also find a mass dependent saturating behavior of $v_2(p_T)$ when semi-hard components are combined with the hydrodynamic components [22].

In summary, we have investigated low- p_T observables in a hadron-string cascade model JAM [21] and a hydrodynamical model [22] in Cu+Cu collisions at $\sqrt{s_{NN}} = 200$ GeV. For $dN/d\eta$ and p_T -spectra for charged hadrons, we have obtained good agreement between JAM and hydrodynamics. However, clear deviations between model predictions are found in v_2 as a function of centrality, pseudorapidity η , and transverse momentum p_T for charged hadrons. A probable interpretation of the result, $v_{2,\text{cascade}} < v_{2,\text{hydro}}$, would be the following: Because of the small size and initial energy density, thermalization is hardly achieved in the non-equilibrium transport calculation, and it gives smaller v_2 than that in hydrodynamics in which complete local thermalization is always assumed. Measurements of pseudorapidity and transverse momentum dependence of elliptic flow ($v_2(b)$, $v_2(\eta)$, and $v_2(p_T)$) in Cu+Cu collisions at RHIC will provide very important information for thermalization and transport aspects of QCD matter in heavy ion collisions.

One of the authors (Y.N.) acknowledges discussions with M. Bleicher. The work was supported in part by the US-DOE under Grant No. DE-FG02-93ER40764 (T.H.), and by the Grant-in-Aid for Scientific Research (No. 1554024) from the Ministry of Education, Science and Culture, Japan.

-
- [1] F. Karsch, Lect. Note Phys. **583**, 209 (2002).
 - [2] M. Gyulassy, I. Vitev, X. N. Wang, and B. W. Zhang, in *Quark Gluon Plasma 3*, edited by R.C. Hwa and X.N. Wang (World Scientific, Singapore, 2004); A. Kovner and U. A. Wiedemann, in *Quark Gluon Plasma 3*, edited by R.C. Hwa and X.N. Wang (World Scientific, Singapore, 2004).
 - [3] R. J. Fries, J. Phys. G **30**, S853 (2004).
 - [4] A. Andronic *et al.* [FOPI Collaboration], Nucl. Phys. A **661**, 333 (1999); Phys. Rev. C **67**, 034907 (2003).
 - [5] P. Chung *et al.* [E895 Collaboration], Phys. Rev. C **66**, 021901 (2002).
 - [6] H. Appelshauser *et al.* [NA49 Collaboration], Phys. Rev. Lett. **80**, (1998) 4136,
 - [7] K. H. Ackermann *et al.* [STAR Collaboration], Phys. Rev. Lett. **86** (2001) 402; C. Adler *et al.* [STAR Collaboration], Phys. Rev. Lett. **87** (2001), 182301; C. Adler *et al.* [STAR Collaboration], Phys. Rev. C **66** (2002), 034904; K. Adcox *et al.* [PHENIX Collaboration], Phys. Rev. C **69** (2004), 024904. B. B. Back *et al.* [PHOBOS Collaboration], Phys. Rev. Lett. **89** (2002) 222301; L. G. Bearden *et al.* [BRAHMS Collaboration], Phys. Lett. B **523** (2001) 227.
 - [8] P. Danielewicz, R. Lacey, W. G. Lynch, Science **298**, 1592 (2002).
 - [9] A. B. Larionov, W. Cassing, C. Greiner and U. Mosel, Phys. Rev. C **62**, 064611 (2000).
 - [10] M. Isse, A. Ohnishi, N. Otuka, P. K. Sahu, Y. Nara, arXiv:nucl-th/0502058.
 - [11] M. Bleicher and H. Stöcker, Phys. Lett. B **526**, 309 (2002).
 - [12] E. L. Bratkovskaya, W. Cassing and H. Stöcker, Phys. Rev. C **67**, 054905 (2003).
 - [13] W. Cassing, K. Gallmeister and C. Greiner, Nucl. Phys. A **735**, 277 (2004).
 - [14] P. K. Sahu, N. Otuka, A. Ohnishi, arXiv:nucl-th/0206010 (2002); P. K. Sahu, A. Ohnishi, M. Isse, N. Otuka, S. C. Phatak, submitted to J. Phys. G (2005).

- [15] G. Baur, J. Bleibel, C. Fuchs, A. Faessler, L. V. Bravina and E. E. Zabrodin, arXiv:nucl-th/0411117.
- [16] Z. Lin, C. M. Ko, Phys. Rev. C **65**, 034904 (2002).
- [17] P. F. Kolb, P. Huovinen, U. W. Heinz and H. Heiselberg, Phys. Lett. B **500**, 232 (2001); P. Huovinen, P. F. Kolb, U. W. Heinz, P. V. Ruuskanen and S. A. Voloshin, Phys. Lett. B **503**, 58 (2001); P. F. Kolb, U. W. Heinz, P. Huovinen, K. J. Eskola and K. Tuominen, Nucl. Phys. A **696**, 197 (2001); P. Huovinen, arXiv:nucl-th/0505036.
- [18] T. Hirano, Phys. Rev. C **65**, 011901 (2002).
- [19] http://www.bnl.gov/bnlweb/pubaf/pr/PR_display.asp?prID=05-38
- [20] T. Hirano and M. Gyulassy, arXiv:nucl-th/0506049.
- [21] Y. Nara, N. Otuka, A. Ohnishi, K. Niita, and S. Chiba, Phys. Rev. C **61**, 024901 (2000).
- [22] T. Hirano and Y. Nara, Nucl. Phys. A **743**, 305 (2004).
- [23] X. -N. Wang and M. Gyulassy, Phys. Rev. D **44**, 3501 (1991).
- [24] T. Sjöstrand *et al.*, Comp. Phys. Comm. **135**, 238 (2001).
- [25] S. A. Bass *et al.*, Prog. Part. Nucl. Phys. **41**, 255 (1998).
- [26] L. D. McLerran and R. Venugopalan, Phys. Rev. D **49**, 2233 (1994); **49**, 3352 (1994); **50**, 2225 (1994).
- [27] E. Iancu and R. Venugopalan, in *Quark Gluon Plasma 3*, edited by R.C. Hwa and X.N. Wang (World Scientific, Singapore, 2004, p249).
- [28] D. Kharzeev and M. Nardi, Phys. Lett. B **507**, 121 (2001); D. Kharzeev and E. Levin, *ibid.* B **523**, 79 (2001); D. Kharzeev, E. Levin, and M. Nardi, arXiv:hep-ph/0111315; D. Kharzeev, E. Levin and M. Nardi, Nucl. Phys. A **730**, 448 (2004).
- [29] P. Huovinen, in *Quark Gluon Plasma 3*, edited by R.C. Hwa and X.N. Wang (World Scientific, Singapore, 2004, p600), arXiv:nucl-th/0305064; P. F. Kolb and U. Heinz, *ibid.*, p634, arXiv:nucl-th/0305084; T. Hirano, Acta Phys. Polon. B **36**, 187 (2005).
- [30] M. Gyulassy, P. Lévai, and I. Vitev, Nucl. Phys. **B594**, 371 (2001); **B571**, 197 (2000); Phys. Rev. Lett. **85**, 5535 (2000); in *Quark Gluon Plasma 3*, edited by R.C. Hwa and X.N. Wang (World Scientific, Singapore, 2004, p123).
- [31] T. Hirano and Y. Nara, Phys. Rev. C **66**, 041901 (2002); T. Hirano and Y. Nara, Phys. Rev. Lett. **91**, 082301 (2003); T. Hirano and Y. Nara, Phys. Rev. C **68**, 064902 (2003); T. Hirano and Y. Nara, Phys. Rev. C **69**, 034908 (2004).
- [32] T. Hirano and K. Tsuda, Phys. Rev. C **66**, 054905 (2002).
- [33] D. Teaney, arXiv:nucl-th/0204023.
- [34] D. Teaney, J. Lauret and E. V. Shuryak, Phys. Rev. Lett. **86**, 4783 (2001); D. Teaney, J. Lauret and E. V. Shuryak, arXiv:nucl-th/0110037.
- [35] C. M. Hung and E. V. Shuryak, Phys. Rev. C **57**, 1891 (1998).
- [36] J. Adams *et al.* [STAR Collaboration], Phys. Rev. Lett. **92**, 112301 (2004).
- [37] B. B. Back *et al.* [PHOBOS Collaboration], Phys. Rev. Lett. **89** (2002) 222301.
- [38] L. -W. Chen and C. M. Ko, arXiv:nucl-th/0505044.